INTERFACE

royalsocietypublishing.org/journal/rsif

Research

Cite this article: Vadlamani RA, Nie Y, Detwiler DA, Dhanabal A, Kraft AM, Kuang S, Gavin TP, Garner AL. 2019 Nanosecond pulsed electric field induced proliferation and differentiation of osteoblasts and myoblasts. *J. R. Soc. Interface* **16**: 20190079.
http://dx.doi.org/10.1098/rsif.2019.0079

Received: 6 February 2019
Accepted: 28 May 2019

Subject Category:
Life Sciences – Engineering interface

Subject Areas:
biomedical engineering, biotechnology, biophysics

Keywords:
electroporation, stem cells, differentiation, proliferation, myoblasts, osteoblasts

Author for correspondence:
Allen L. Garner
e-mail: algarner@purdue.edu

Electronic supplementary material is available online at https://dx.doi.org/10.6084/m9.figshare.c.4531235.

THE ROYAL SOCIETY PUBLISHING

Nanosecond pulsed electric field induced proliferation and differentiation of osteoblasts and myoblasts

Ram Anand Vadlamani[1], Yaohui Nie[2], David A. Detwiler[6], Agni Dhanabal[3], Alan M. Kraft[1], Shihuan Kuang[4], Timothy P. Gavin[2] and Allen L. Garner[1,3,5]

[1]School of Nuclear Engineering, [2]Department of Health and Kinesiology, [3]Department of Agricultural and Biological Engineering, [4]Department of Animal Sciences, and [5]School of Electrical and Computer Engineering, Purdue University, West Lafayette, IN 47907, USA
[6]Nanovis, Inc., West Lafayette, IN 47907, USA

AD, 0000-0002-8916-3425; ALG, 0000-0001-5416-7437

Low-intensity electric fields can induce changes in cell differentiation and cytoskeletal stresses that facilitate manipulation of osteoblasts and mesenchymal stem cells; however, the application times (tens of minutes) are of the order of physiological mechanisms, which can complicate treatment consistency. Intense nanosecond pulsed electric fields (nsPEFs) can overcome these challenges by inducing similar stresses on shorter timescales while additionally inducing plasma membrane nanoporation, ion transport and intracellular structure manipulation. This paper shows that treating myoblasts and osteoblasts with five 300 ns PEFs with intensities from 1.5 to 25 kV cm^{-1} increased proliferation and differentiation. While nsPEFs above 5 kV cm^{-1} decreased myoblast population growth, 10 and 20 kV cm^{-1} trains increased myoblast population by approximately fivefold 48 h after exposure when all cell densities were set to the same level after exposure. Three trials of the PEF-treated osteoblasts showed that PEF trains between 2.5 and 10 kV cm^{-1} induced the greatest population growth compared to the control 48 h after treatment. Trains of nsPEFs between 1.5 and 5 kV cm^{-1} induced the most nodule formation in osteoblasts, indicating bone formation. These results demonstrate the potential utility for nsPEFs to rapidly modulate stem cells for proliferation and differentiation and motivate future experiments to optimize PEF parameters for *in vivo* applications.

1. Introduction

While stem cell therapies hold great promise, several challenges remain for clinical translation, including appropriate maintenance of stem cell state, reproducibly expanding large numbers of stem cells for transplantation, assuring efficient differentiation into desired cell types and ensuring cell viability during and after delivery [1]. For example, the slow proliferation of myoblasts and osteoblasts until differentiation significantly hinders clinical applications for muscular and bone regeneration [2,3]. Inducing differentiation may benefit certain applications, such as bone healing and regeneration [3–5]. This has motivated multiple physical methods, including mechanical and electrical stimulation [6], and chemical methods, such as substrate and materials design [7], to control and direct stem cell differentiation and proliferation. Electric fields are increasingly used as an alternative to drugs or gene therapy for treatment and regeneration due to their ease of use and ability to induce desirable phenomena [4,5]. Electric fields can control differentiation by modifying the membrane potential [8,9], which impact voltage-gated channels [10] and the influx of ions to determine the differentiation of embryonic stem cells [11]. Electric fields can also induce cytoskeletal stresses to manipulate osteoblasts and mesenchymal stem cells [12], which was previously possible only by using chemicals [13] or proteins [14].

Many studies exploring the electric field and electromagnetic stimulation of stem cells consider long duration, low-intensity electric [15] or magnetic fields [16,17]. These long duration mechanisms may be challenging to apply consistently because the physical interactions may conflict with long-term physiological mechanisms at similar voltages and currents [18]. For instance, applying a single pulsed electric field (PEF) 2.5 V cm^{-1} of 90 s duration altered cardiomyocyte differentiation by increasing the number of beating foci while applying a single 5.0 V cm^{-1} PEF additionally increased intracellular reactive oxygen species [19,20]. A more recent study examined the application of picosecond PEFs to manipulate the proliferation and lineage-specific gene expression in neural stem cells [21].

Although the effect of these electric fields on osseointegration is incompletely characterized [5], recent studies have shown that electrical stimulation can enhance bone growth. Applying voltages under 500 mV to the titanium surfaces used in implants clinically promoted bone regeneration for fractures by enhancing osteoblast differentiation [22]. Applying degenerate sine-wave and capacitively coupled stimulation for 4 h increased differentiation and mineralization and collagen production of osteoblast-like cells *in vitro* [23]. Electrical stimulation increased the growth of adipose-derived mesenchymal stem cells in conductive scaffolds by manipulating voltage-gated calcium, sodium and potassium channels [24].

Adult skeletal muscle demonstrates an efficient regenerative capacity in response to physiological stimulus, such as intense exercise and muscle injury, by activating resident stem cells (satellite cells) in a mediated myogenic programme [25]. These cells remain quiescent between the basal lamina and the plasma membrane of the myofibres until activated by regenerative signals. Once stimulated, these satellite cells undergo multiple rounds of divisions, differentiation and fusion to form new multinucleated myofibres, which is critical for postnatal maintenance of skeletal muscle and muscle repair. Ageing muscles exhibit impaired regenerative ability, partly due to a loss of stem cell populations and increased defects in satellite cells [26].

The current study experimentally assesses the impact of nanosecond PEFs (nsPEFs) on osteoblast and myoblast proliferation and differentiation. Applying nsPEFs avoids some potential challenges of low-voltage electric fields by applying decisively non-physiological parameters (electric fields of 30–300 kV cm^{-1} and pulse durations of 10–300 ns) to induce various physical mechanisms, such as plasma membrane nanoporation, ion transport and intracellular structure manipulation [27]. Applying nsPEFs can induce these phenomena with minimal tissue heating and the ability to target intracellular structures, such as calcium stores [28] and the cytoskeleton [29]. While further research is needed to determine their influence on gene expressions and growth factors, the appropriate tuning of intense PEFs provides the potential to provide both mechanical and electrical stresses [30] to facilitate adequate microenvironment control to manipulate stem cell function.

While nsPEFs have been used for treatment before, such as inactivating microorganisms [31,32] and activating apoptotic pathways in melanomas [33], this study examines the application of nsPEFs with a lower cumulative energy density on stem cell stimulation [11,19,34]. Electric field intensity can dramatically impact mechanism. Recent studies using electrostimulation with capacitive coupling (indirect contact with a sample) induced similar levels of haematopoietic and mesenchymal stem cell activation as bovine thrombin, the state of the art platelet activator, while conductive coupling (direct contact with the sample) increased cell death [35]. Although the applied voltage was the same, capacitive coupling induces a much lower membrane potential than conductive coupling [36], creating less intense biophysical effects. In general, applying greater pulse energy (more pulses, higher electric field or longer pulse duration) induces cell death [37,38].

The current study assesses the feasibility of selecting nsPEF parameters to stimulate osteoblast and myoblast behaviour without inducing adverse effects, such as cell death, much as PEFs are applied for platelet activation [39]. While applying nsPEFs allows for a lower duty cycle and application of higher electric fields [37], this study demonstrates that applying only five electric pulses from 2.5 to 5 kV cm^{-1} could stimulate osteoblasts and myoblasts with potential implications to regenerative healing and tissue repair. Section 2 summarizes the material and methodology. Section 3 reports the results. We discuss the results and provide concluding remarks in §4.

2. Material and methodology

2.1. Isolation and culture of primary myoblasts

Primary myoblasts were isolated from hindlimb skeletal muscle of four-week-old mice [40] (PMID: 27880908). Briefly, muscles were minced and digested in type B collagenase and dispase II mixture (Roche). Digested cells were harvested and cultured in growth media, F-10 Ham's medium (Thermo Fisher Scientific) supplemented with 20% fetal bovine serum (FBS, Atlanta), 4 ng ml^{-1} basic fibroblast growth factor (Thermo Fisher Scientific) and 1% penicillin–streptomycin (Thermo Fisher Scientific) on collagen-coated dishes. Primary myoblasts were isolated and purified after preplating two to three times. Primary myoblasts were then induced to differentiate by growing in Dulbecco's modified Eagle's medium (DMEM, Sigma,) supplemented with 2% horse serum (Sigma) for at least 2 days.

2.2. Culture of primary human osteoblasts

Primary human osteoblasts obtained from vertebrae (Sciencell®) were cultured in DMEM/F-12 media (Gibco) supplemented with 10% FBS with 1% L-glutamine + 1% penicillin–streptomycin antibiotic in tissue culture grade flasks. Cells were removed from the adhered surface and concentrated to 2×10^6 cells ml^{-1} prior to pulsing in a 2 mm gap cuvette. These were then plated in 96-well plates with a methyl thiazolyl tetrazolium (MTT) stain to take counts 4, 24 and 48 h after nsPEF treatment, followed by plating cells at 1×10^4, 2.5×10^4 and 5×10^4 cells $well^{-1}$ in a 24-well plate for immunostaining prior to fluorescence studies.

2.3. Nanosecond pulsed electric field exposure

To maintain consistent stem cell regenerative capacity, we used myoblasts between the second and eighth passage for all experiments. Myoblasts were cultured in 10 cm dishes until achieving 80% confluency. Similarly, osteoblasts were passaged for pulsing upon reaching 80% confluency. Both samples were diluted to a concentration of 2×10^6 cells ml^{-1},

placed in standard 2 mm electroporation cuvettes (Dot Scientific®) and treated by a 300 ns PEF using a pulse generator consisting of 24 capacitors and inductors arranged as a standard Blumlein circuit design [41]. The pulse generator was powered by an EJ series Glassman® high voltage 600 W DC power supply and activated with a spark gap switch to produce PEFs of 300 ns duration at the peak with rise and fall times of approximately 30 ns. Each treatment exposed the samples to five pulses at a repetition frequency of 1 Hz. The absence of asymmetric bipolar pulses when applying PEFs to growth media and PBS indicates that the load approximately matches the pulse generator's impedance of 10 Ω. We measured the applied voltage across the cuvette using a LeCroy PPE 20 kV high-voltage probe with a 1000 : 1 attenuation that fed into a TeleDyne LeCroy® Waverunner 6 Zi Oscilloscope capable of measuring up to 4 GHz. Figure 1 shows a typical measured waveform. We report the electric field across the parallel plates as $E = V/d$, where V is the peak voltage of the applied PEF in kV and d is the gap distance in cm (0.2 cm here).

2.4. Plating after pulsed electric field treatment

Immediately after treating the myoblasts with five PEFs, we used a haemocytometer to determine the number of viable, surviving cells (cf. figure 2*a*) to ensure we plated the same number of live cells in each well. The viability counts were obtained using a Trypan blue exclusion assay on an automated cell counter, the Invitrogen® Countess 2, set to read cells up to 80 µm in diameter. Seeding the wells with the same cell density required diluting the samples and accounting for cell death to ensure the plating of 2×10^4 live cells per well. This resulted in figure 2*a*, which includes haemocytometer counts ($n = 5$), with the lower intensity PEFs inducing minimal effect and more intense PEFs causing approximately a 40% reduction in the number of viable cells. Three wells each were used for MTT assays at 24 and 48 h after pulsing in 96-well plates.

Similarly, osteoblasts were treated with five pulses, but plated at the same volume of cell solution, using the control as a reference. The control (unpulsed) sample contained 2×10^4 live cells in 10 µl of fluid. The same volume was plated for all treated samples to better simulate clinical conditions/applications. The cells were plated in three wells for each condition in 24-well plates in a total volume of 200 µl. Counts were taken 4, 24 and 48 h after plating with 4 h selected as the initial time to ensure sufficient time for the cells to adhere to the cell wall surface.

2.5. Cell proliferation assay

Cell proliferation was assessed by using the MTT cell proliferation assay kit from ATCC (ATCC 30–1010 K). Experiments consisted of adding 10 µl of 5 mg ml^{-1} MTT to each well of the 96-well plates containing pulsed cells at 0, 24 and 48 h after treatment. We drained the media 4 h after incubation at 37°C for the initial (0 h) count to allow adherence to the dish surface. Purple formazan dyes were dissolved in 100 µl DMSO in each well and absorbance was measured at 570 nm for the myoblast experiments.

For osteoblasts, we drained the media 1 h prior to counting and added a mixture of 100 µl media and 20 µl MTT to each well, which was allowed to stain for 1 h. Next, 100 µl of the stained solution was transferred from each well to a 96-well plate to count with a photospectrometer at a wavelength of 570 nm.

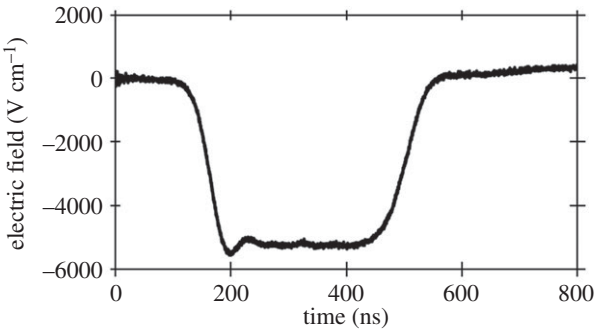

Figure 1. Electric field for a representative 300 ns pulse produced by the pulse generator across a 0.2 cm cuvette by using $E = V/D$ with V the applied voltage and D the cuvette gap.

2.6. Immunofluorescence

Pulsed myoblast cells were seeded in 24-well plates of 15.6 mm diameter and 3.4 ml volume at a density of 3×10^5 cells well^{-1}. After 48 h, the cells were cultured in growth media or differentiation media for 72 h. After removing the media, we fixed the cells in 4% paraformaldehyde (PFA) for 5 min and incubated in 100 mM glycine for 15 min. Cells were then permeabilized in blocking buffer containing 5% goat serum, 2% bovine serum albumin, 0.2% Triton X-100 and 0.1% sodium azide in PBS for 1 h. Myosin heavy chain protein was used as the maturation marker of myoblasts. The primary antibody MF20 (R&D Systems®, #MAB4470, mouse) was added to the blocking buffer in a 1 : 30 dilution and applied to cells overnight at 4°C. Cells were then incubated in an anti-mouse IgG2b 568 (Invitrogen) secondary antibody for 1 h and cell nuclei were co-stained with 1 µM DAPI. We captured between four and six fluorescent images per well with a CoolSnap HQ charge coupled-device camera (Photometrics) and a Leica DM6000 microscope. Figure 3 shows representative images from different wells. Because the instrumentation did not permit application of a 'scale' or 'ruler' for relative size, these images provide insight into the occurrence of differentiation but prohibit quantitative assessments. Future studies using confocal microscopy will enable quantification of these results.

2.7. Osteoblast staining

Osteoblasts were fixed in 0.5% glutaraldehyde solution in phosphate-buffered saline for 1 h. Cultures were rinsed with deionized water and stained with Alizarin Red stain, 40 mM in deionized water pH 4.2 (Sigma A5533). Stain was placed on cultures for 1 h with agitation. Cultures were destained with repeated deionized water rinses for 24 h.

2.8. Statistical analysis

To confirm the myoblast results for initial cell kill off after pulsing and proliferation 24 h and 48 h after PEF treatment, we performed a repeated measure analysis of variance (ANOVA) followed by a Tukey test for multiple comparisons if the ANOVA showed a significant difference for the independent variable ($p < 0.05$). We present the results by letter with conditions sharing a letter exhibiting no statistically

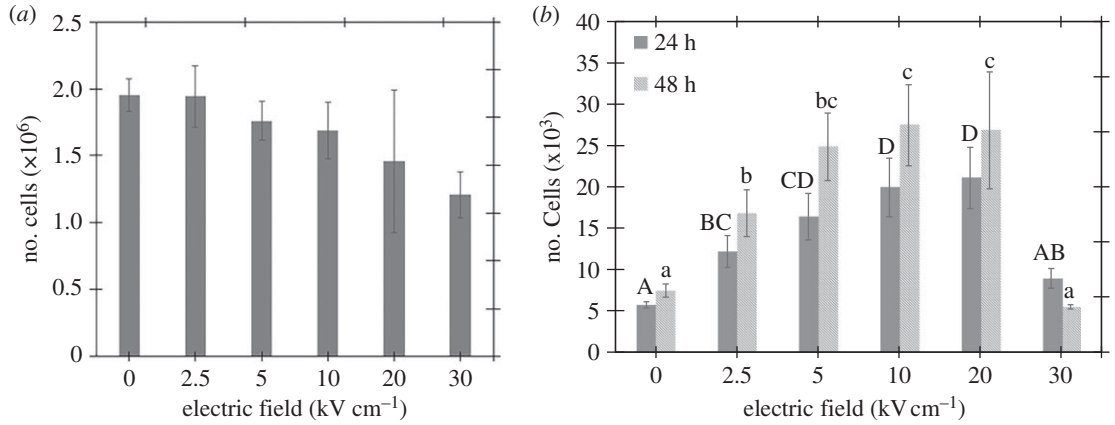

Figure 2. (*a*) Myoblast count immediately after treatment to plates with an identical number of cells in each well. (*b*) Myoblast population determined by MTT assays 24 and 48 h after five 300 ns PEFs. The Tukey groupings are labelled above each column to compare the treatments showing a significant difference ($p < 0.05$). In all cases, the electric field is calculated as $E = V/D$, where V is the applied voltage and D is the gap distance of the cuvette (0.2 cm).

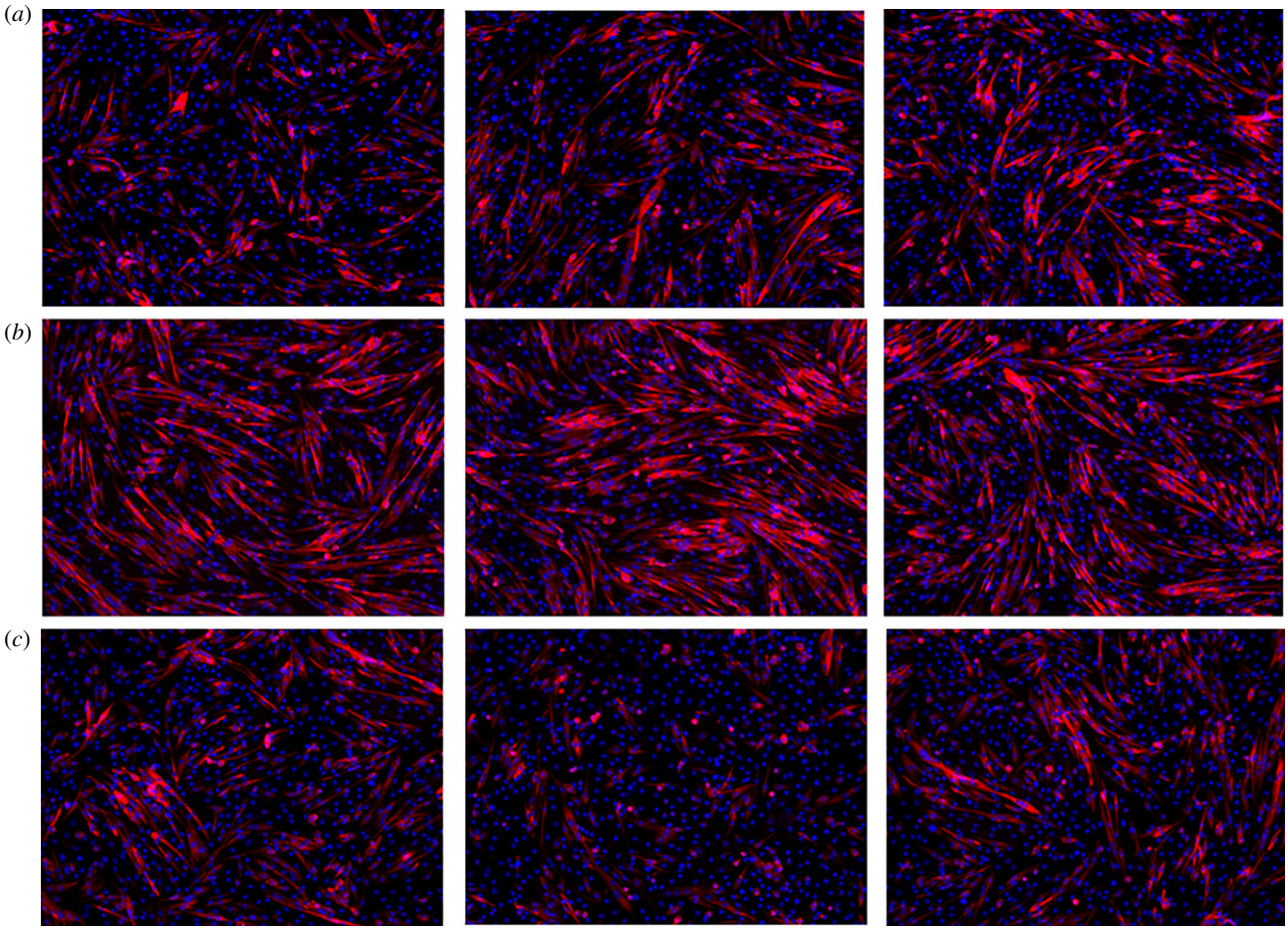

Figure 3. Representative immunostaining images from portions of three different wells of untreated myoblasts (*a*) and myoblasts following exposure to five 5 kV cm^{-1} (*b*) or 25 kV cm^{-1}, 300 ns (*c*) PEFs. The red and blue mark the myosin heavy chains and cell nuclei, respectively. The myoblasts treated with 5 kV cm^{-1} have a larger concentration of red cells, indicating increased proliferation. These images show that the 25 kV cm^{-1} treatment induced less myoblast fusion compared to the control and the 5 kV cm^{-1} field treatment. (Online version in colour.)

significant difference and those not sharing a letter having a statistically significant difference. For example, if group 1 is assigned 'AB', group 2 is assigned 'B', and group 3 is assigned 'A', then group 1 is not statistically different from group 2 or 3 because it shares a letter with each group, but groups 2 and 3 are statistically different as they do not share the same letter.

3. Results

3.1. Myoblast results

Myoblasts were treated with five 300 ns PEFs at 0, 2.5, 5, 10, 20 or 30 kV cm^{-1}. Figure 2*a* shows that the number of cells was unchanged at 2.5 kV cm^{-1} and decreased with increasing PEF field strength from 5 to 30 kV cm^{-1}. Figure 2*a*

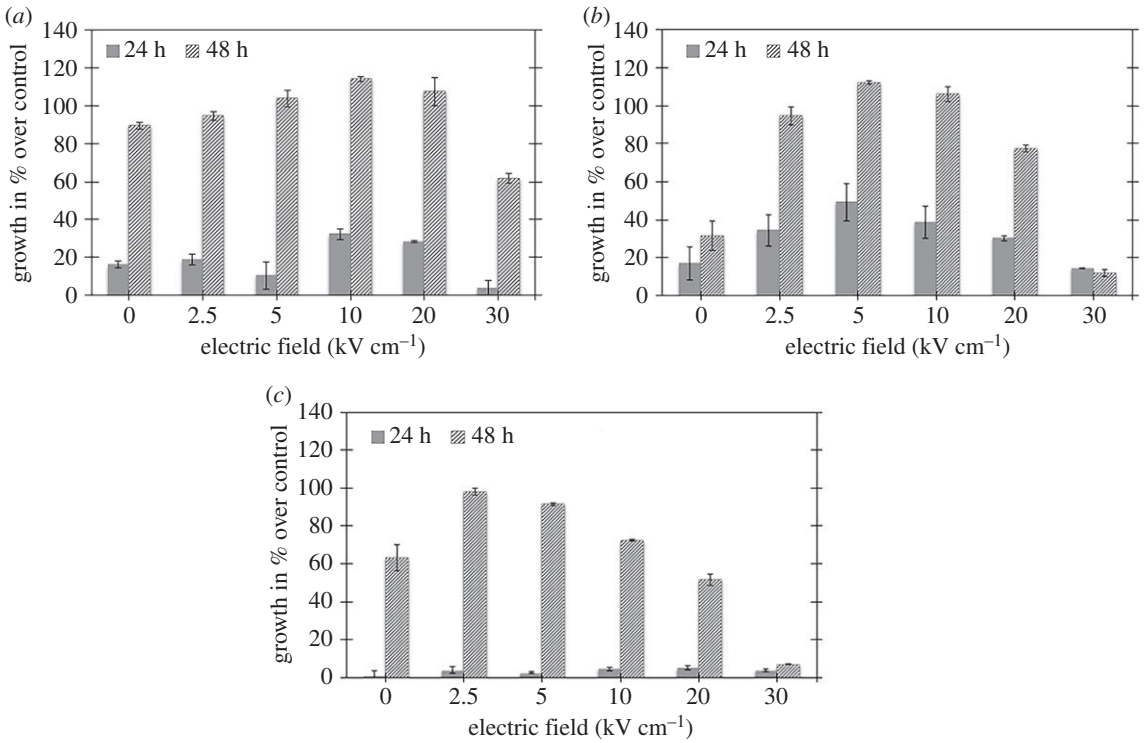

Figure 4. Osteoblast proliferation 0, 24 and 48 h as a percentage of the initial untreated control population after treatment with 300 ns PEFs with various intensities for three different trials demonstrating increased proliferation compared to untreated control (0 kV cm^{-1}) for electric fields from (*a*) 10 to 20 kV cm^{-1} at 24 h and 2.5 to 20 kV cm^{-1} at 48 h, (*b*) 2.5 to 20 kV cm^{-1} at 24 h and 2.5 to 20 kV cm^{-1} at 48 h and (*c*) 2.5 to 10 kV cm^{-1} at 48 h after treatment. In all cases, the electric field is calculated as $E = V/D$, where V is the applied voltage and D is the gap distance of the cuvette (0.2 cm).

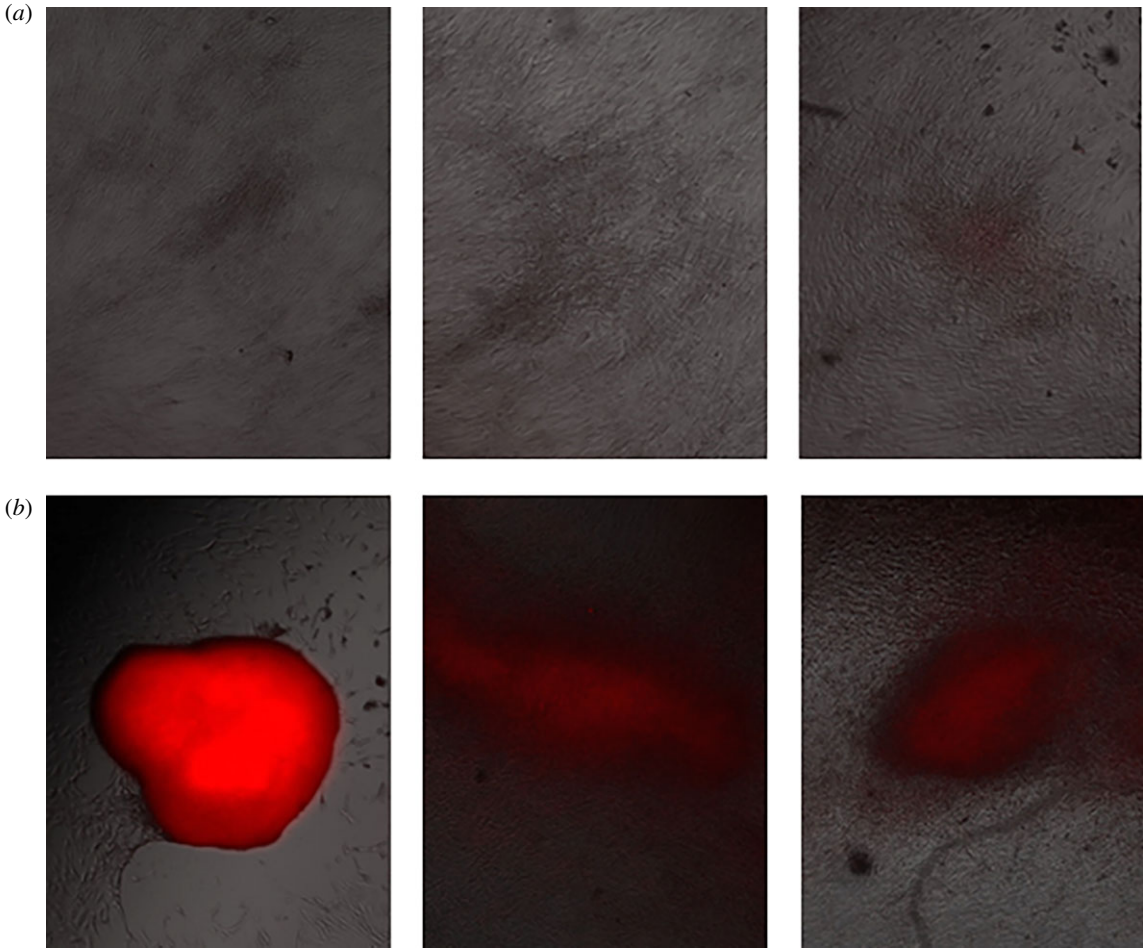

Figure 5. Representative fluorescent images from each of three wells for untreated osteoblast control cells 7 days (*a*) and 14 days (*b*) after the experiment indicating light nodule formation after 14 days, as indicated by the red coloration. (Online version in colour.)

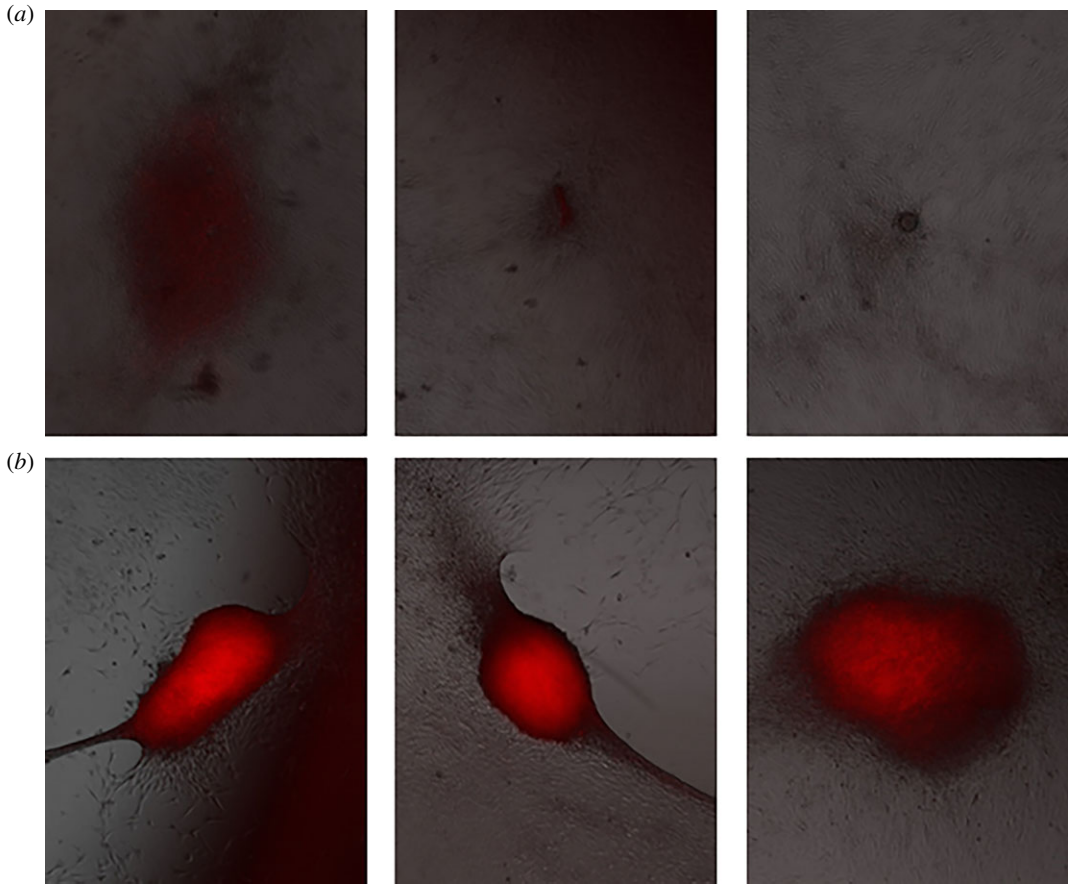

Figure 6. Representative fluorescent images from each of three wells 7 days (*a*) and 14 days (*b*) after treating osteoblast cells with five, 1.5 kV cm^{-1}, 300 ns PEFs 7 days and 14 days indicating enhanced nodule formation after 14 days. (Online version in colour.)

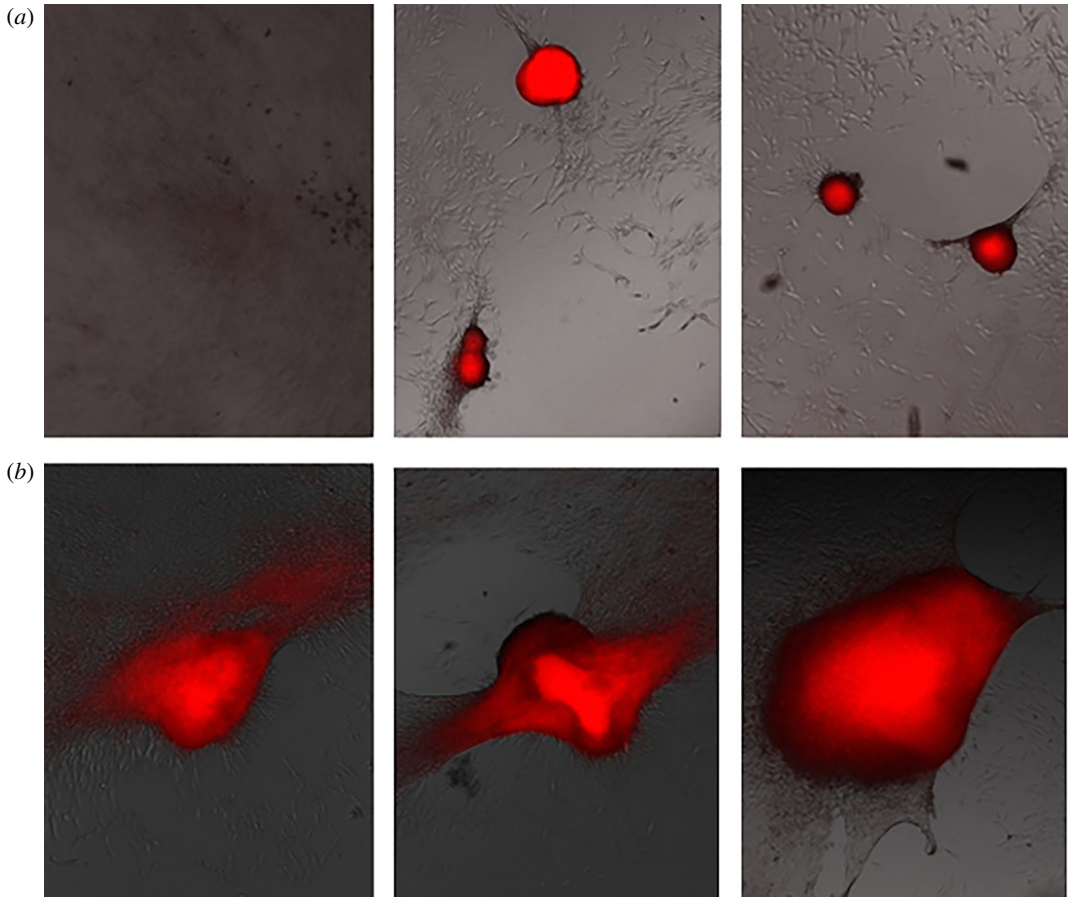

Figure 7. Representative fluorescent images from each of three wells 7 days (*a*) and 14 days (*b*) after treating osteoblast cells with five, 2.5 kV cm^{-1}, 300 ns PEFs indicating nodule formation after 7 days and more extensive nodule formation after 14 days. (Online version in colour.)

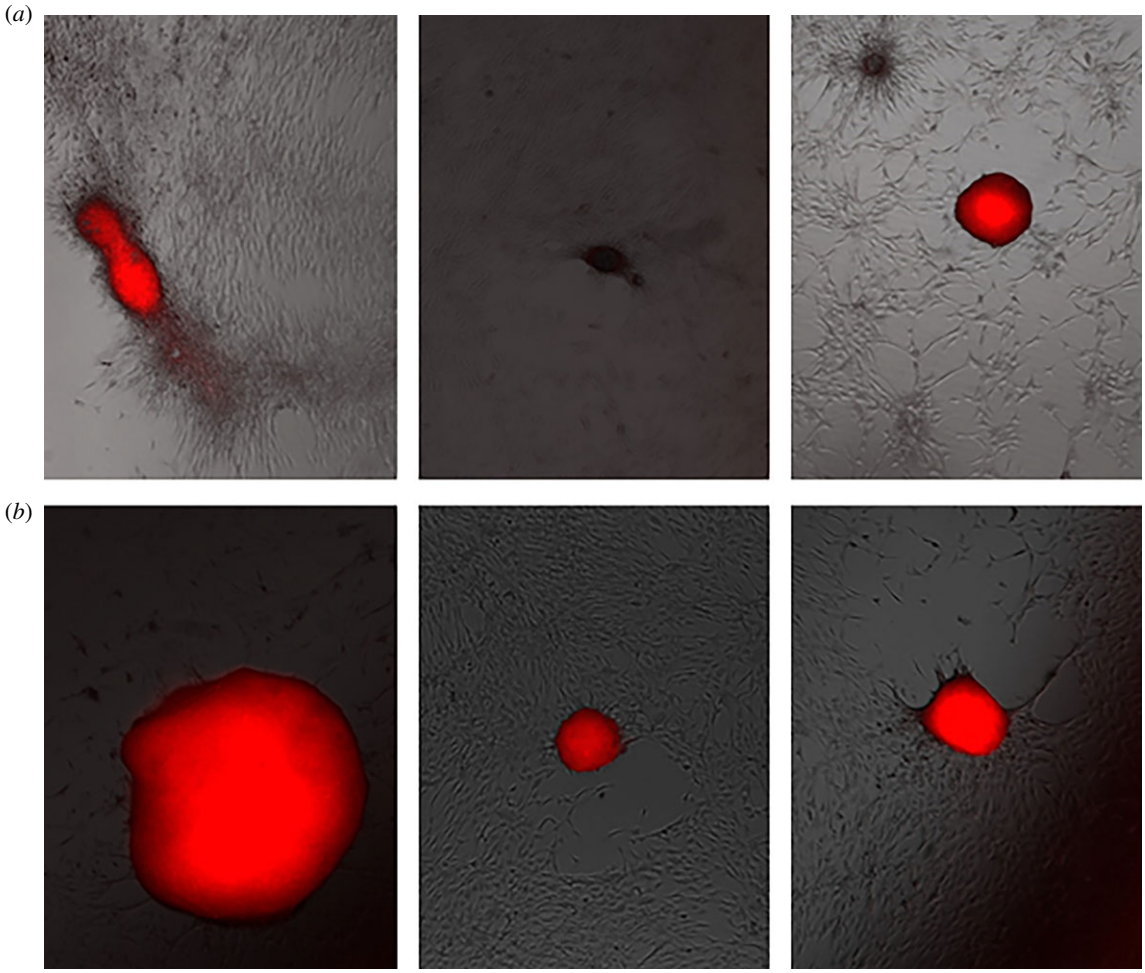

Figure 8. Representative fluorescent images from each of three wells 7 days (*a*) and 14 days (*b*) after treating osteoblast cells with five, 5 kV cm^{-1}, 300 ns PEFs indicating nodule formation after 7 days and more extensive nodule formation after 14 days. (Online version in colour.)

shows that the number of myoblast cells that survived PEF treatment decreased for increased field strengths. Performing an ANOVA on the cell count data in figure 2*a* showed no statistical significance in cell count as a function of electric field intensity ($p = 0.197$).

A fixed volume of cells was then seeded to monitor the growth rate. Figure 2*b* shows that the 2.5 kV cm^{-1} PEFs increase myoblast proliferation by twofold without impairing survival, while the 5, 10 and 20 kV cm^{-1} PEFs increase growth rate by three- to fourfold with a reduced survival rate. Independently running the 24 and 48 h results for ANOVA tests showed that different applied electric field intensities had a statistically significant difference on cell population ($p < 0.001$). A Tukey test was conducted to determine the significance between individual PEF parameters. The growth rate was lower 48 h post-treatment at 30 kV cm^{-1}, suggesting that these PEFs may exceed a threshold for damaging myoblast physiology. The increased proliferation resulted in a high cell density that caused the myoblasts to differentiate spontaneously without the serum withdrawal typically used to induce myoblast differentiation.

Myotube differentiation is the physiological process for myoblast maturation. We studied differentiation 2 days after PEF treatment to assess the impact on myoblast function. Figure 3 shows that replacing the growth media with differentiation media causes more fused myoblasts for 5 kV cm^{-1} PEFs compared to control, as indicated by the presence of the myosin heaven chains (stained in red), the maturation marker in the myotubes. By contrast, fewer fused myoblasts formed at 25 kV cm^{-1}, indicating that lower intensity PEFs (5 kV cm^{-1}) maintained myoblast maturation while higher intensity PEFs may impair myoblast differentiation. We hypothesize that this trend will continue at higher electric fields. The initial plated myoblasts had more myosin heavy chains (stained in red) because they fused with other cells to form multinucleated myotubes (blue highlights the nuclei of the cells). Combined, figure 2 shows that PEF treatment increased cell proliferation compared to the untreated control with each image taken from a different well of a 24-well cell culture dish and figure 3 shows that this increases myoblast differentiation at low PEF intensity (5 kV cm^{-1}) but not at high PEF intensity (25 kV cm^{-1}).

3.2. Osteoblast results

Similarly, we set osteoblast concentration to 2×10^6 cells ml^{-1} prior to pulsing. For the untreated control sample, 10 µl of this sample corresponds to 2×10^4 cells well^{-1}. This same volume of fluid was then plated for all samples in 24-well plates (2 cm^2 well^{-1}). The initial population count was taken using an automated cell counter (Countess®). We performed MTT assays at 4, 24 and 48 h ($n = 3$). We consider the 4 h point as the initial condition for calculating subsequent osteoblast population growth. We report the growth curves for pulsed osteoblasts measured from the MTT assay as a percentage of growth compared to

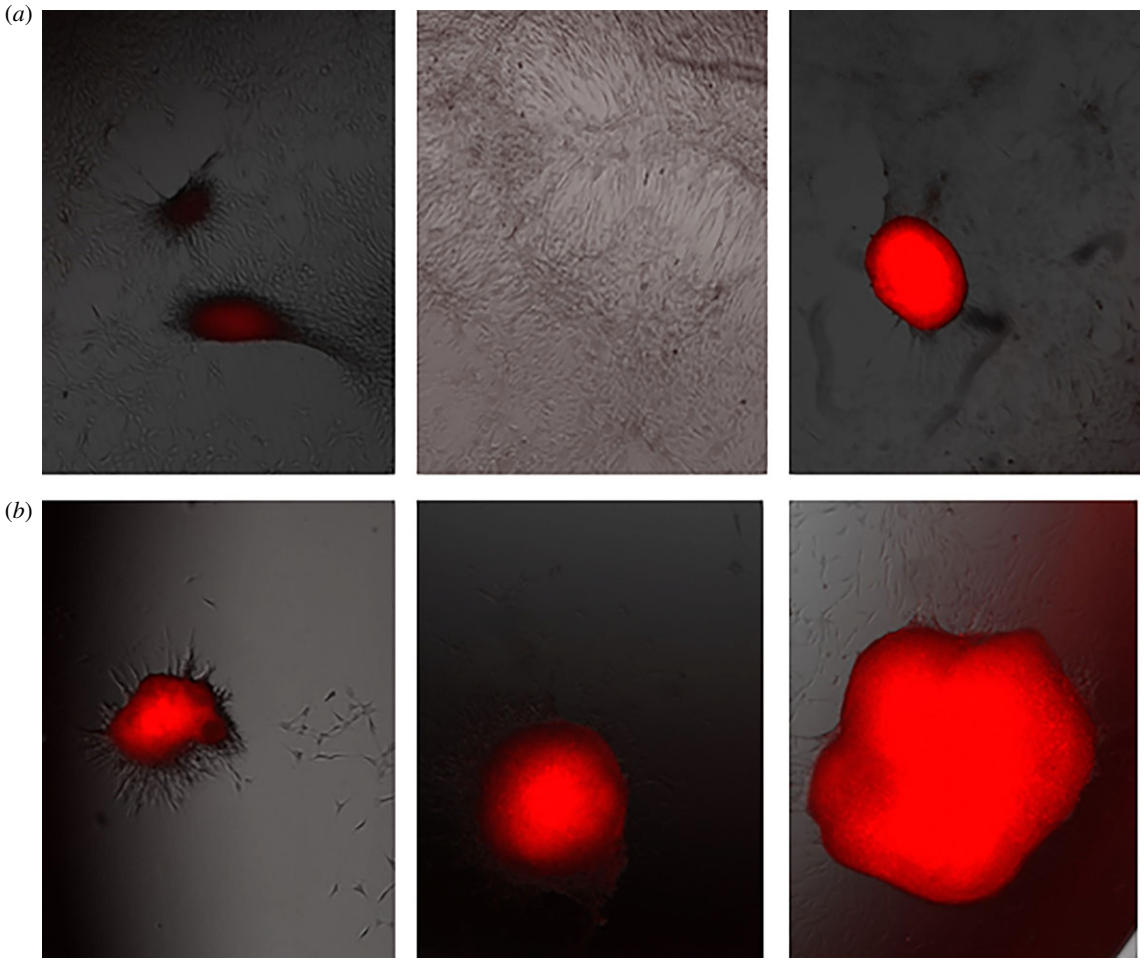

Figure 9. Representative fluorescent images from each of three wells 7 days (*a*) and 14 days (*a*) after treating osteoblast cells with five, 10 kV cm^{-1}, 300 ns PEFs exhibiting nodule formation after 7 days and more extensive nodule formation after 14 days. (Online version in colour.)

the untreated control at 24 and 48 h after treatment. Figure 4 summarizes the results from three identical tests with the exception of the initial osteoblast concentration, which impacts the growth curves after nsPEF exposure. Thus, rather than averaging the results and obtaining large error bars that would hide the general nsPEF behaviour, we report the individual results and observe the general trends.

As with the myoblasts, we plated, stained and photographed the osteoblasts 7 days and 14 days after plating, as shown in figures 5–9 for the untreated control and cells exposed to five 300 ns PEFs at 1.5 kV cm^{-1}, 2.5 kV cm^{-1}, 5 kV cm^{-1} and 10 kV cm^{-1}, respectively. Each figure shows representative images from each of the three wells with the red colour representing nodule formation, which indicates bone formation. While we controlled for the intensity of the red colour, larger red spots indicate greater nodule formation. All field strengths induced notably increased nodule formation 14 days after treatment with treatments of 2.5 kV cm^{-1} and higher inducing some nodule formation even after 7 days. Table 1 reports the nodule counts 14 days after exposing the osteoblasts to five 300 ns PEFs with various intensities and the unpulsed control.

The osteoblast experiments were plated according to the control to reduce the error inherent in counting haemocytometers. We plated 10 µl of each sample into each well, corresponding to the number of live cells of the unpulsed control, which had 2×10^6 cells ml^{-1} with a variation of $\pm 10\%$. This gave 2×10^4 cells (with respect to the untreated control) in each well. The actual large variation in population following PEF exposure may arise due to the variation in the number of cells that survived PEF treatment; however, the trend of increased cell population growth remained. While the variation is sufficient that the results have no statistical significance, we note that the intermediate pulse durations of 1.5 and 2.5 kV cm^{-1} generally lead to the largest increase in nodule formation for each replicate in each trial. No nodules form in the control and only a single nodule forms following the 2.5 kV cm^{-1} treatment in one of the replicates in trial 1. In trial 2, the 2.5 kV cm^{-1} treatment increased nodule formation compared to control in three of the four replicates and by 63.6% compared to control on average, compared to 36.4% and 54.5% for the 3 and 5 kV cm^{-1} treatments, respectively. We also observed notable increases in nodule formation in trial 3 with the 1.5 kV cm^{-1}, all PEF trains below 10 kV cm^{-1} were effective for this trial. As a whole, these data suggest that the 1.5–5 kV cm^{-1} PEF trains are generally effective while nodule formation declines for the 10 kV cm^{-1} trains.

4. Discussion and conclusion

These results indicate that applying five 300 ns PEFs of appropriate electric field intensity to either myoblasts or osteoblasts can induce proliferation and myotube maturation or nodule formation, respectively. For myoblasts, PEFs ranging from 2.5 to 20 kV cm^{-1} increased myoblast population

Table 1. Nodule growth for each replicate of three trials of osteoblasts 14 days after exposure to five 300 ns PEFs of various intensities. Values in italics indicate the average of the quantities in the three rows above.

field (kV cm^{-1})	0	1.5	2.5	5	10
trial 1	0	0	0	0	0
	0	0	1	0	0
	0	0	0	0	0
average	*0.0*	*0.0*	*0.3*	*0.0*	*0.0*
trial 2	2	6	7	7	2
	2	4	3	6	3
	5	3	2	2	3
	2	5	3	2	4
average	*2.8*	*4.5*	*3.8*	*4.3*	*3.0*
trial 3	2	2	5	2	1
	0	3	1	1	0
	0	2	1	1	1
average	*0.7*	*2.3*	*2.3*	*1.3*	*0.7*

compared to untreated control 24 and 48 h after treatment while PEFs above 25 kV cm^{-1} reduced cell population immediately after treatment. The cell population growth does not differ statistically significantly from the control sample. Immunostaining indicated that an applied electric field of 5 kV cm^{-1} increased myotube formation compared to either untreated control or myoblasts exposed to 25 kV cm^{-1}. Thus, an optimal field intensity could selectively enhance myotube formation. We observed similar results for the osteoblasts, including nodule formation within 48–72 h and increased nodule formation for higher field strengths.

Thus, the immunostaining images revealed increased proliferation after pulsing either cell type, which could contribute to increased cell differentiation. Prior research [3] showed that electric field induced ion movement could create currents that affected transmembrane voltage, which can determine the differentiation pathway of mesenchymal stem cells [5]. The release of intracellular stores of Ca^{2+} can also affect growth kinetics. Refs. [4] and [5] show that electrical stimulation can enhance osteoblast differentiation by altering the transmembrane potential, which subsequently influences growth and differentiation. Since nsPEFs target the plasma membrane, intracellular organelle membranes, intracellular calcium stores and the cytoskeleton [27], it is likely that a similar release of stored intracellular ions and the inhibition or activation of other signalling pathways stimulated population growth and differentiation. PEFs may also alter the transmembrane potential [42], providing another potential avenue for stem cell manipulation. Future detailed biological studies examining various markers and mechanisms may elucidate the dominant mechanisms to potentially enable tuning of the phenomenon.

Future tests combining differentiating and non-differentiating media with nsPEFs can determine whether this synergistically increases differentiation, analogous to our past studies assessing the synergy of antimicrobial agents with nsPEFs [43]. Polymerase chain reaction (PCR) tests can analyse changes in mRNA and the transcriptome that could indicate whether nsPEFs induce differentiation. Moreover, the current study focuses on just the impact of applied pulse energy by controlling the applied electric field; however, one could also vary the PEF duration, number of PEFs and even the delivery mechanism from conductive coupling to capacitive coupling. Future studies will involve performing a more detailed parametric study of PEF parameters, which will impact cellular target and intensity, and further assessing the impact of PEFs on membrane potential and calcium release. Ultimately, animal studies can demonstrate the utility of this approach for clinical applications in wound healing.

Ethics. This article does not contain any studies with human participants. The mouse cells were extracted under Purdue Animal Care and Use Committee (PACUC) approval.

Data accessibility. Data are available as electronic supplementary material.

Authors' contributions. The study was conceived and experiments were planned by R.A.V., Y.N., D.A.D. and A.L.G. Experiments were performed and data were collected by R.A.V., Y.N., D.A.D. and A.D. The microscopy work was done by Y.N., R.A.V., A.D. and A.M.K. Analysis of data was done by R.A.V. based on inputs from all authors, including S.H.K., T.P.G. and A.L.G. The article was drafted by R.A.V., D.A.D. and A.L.G. and was critically revised by all authors.

Competing interests. D.A.D. is an employee of Nanovis, Inc.

Funding. This work was supported by the U.S. Nuclear Regulatory Commission Nuclear Education Program Faculty Development Grant Program at Purdue University (grant number NRC-HQ-84-14-G-0048). Nanovis, Inc. provided materials.

References

1. Madl CM, Heilshorn SC, Blau HM. 2018 Bioengineering strategies to accelerate stem cell therapeutics. *Nature* **557**, 335–342. (doi:10.1038/s41586-018-0089-z)
2. Golberg A, Bei M, Sheridan RL, Yarmush ML. 2013 Regeneration and control of human fibroblast cell density by intermittently delivered pulsed electric fields. *Biotechnol. Bioeng.* **110.6**, 1759–1768. (doi:10.1002/bit.24831)
3. Su C-Y, Fang T, Fang H-W. 2017 Effects of electrostatic field on osteoblast cells for bone regeneration applications. *BioMed Res. Int.* **2017**, 7124817. (doi:10.1155/2017/7124817)
4. Eswaramoorthy SD, Bethapudi S, Almelkar SI, Rath SN. 2018 Regional differentiation of adipose-derived stem cells proves the role of constant electric potential in enhancing bone healing. *J. Med. Biol. Eng.* **38**, 804–815. (doi:10.1007/s40846-018-0373-2)
5. Khalifeh JM, Zohny Z, Gamble P, MacEwan M, Ray WZ. 2018 Electrical stimulation and bone healing: a review of current technology and clinical applications. *IEEE Rev. Biomed. Eng.* **11**, 217–232. (doi:10.1109/RBME.2018.2799189)
6. Handschin C, Mortezavi A, Plock J, Eberli D. 2015 External physical and biochemical stimulation to enhance skeletal muscle bioengineering. *Adv. Drug Deliv. Rev.* **82**, 168–175. (doi:10.1016/j.addr.2014.10.021)
7. Schmidt S, Lilienkampf A, Bradley M. 2018 New substrates for stem cell control. *Phil. Trans. R. Soc. B* **373**, 20170223. (doi:10.1098/rstb.2017.0223)
8. Sundelacruz S, Levin M, Kaplan DL. 2008 Membrane potential controls adipogenic and osteogenic differentiation of mesenchymal stem cells. *PLoS ONE* **3**, e3737. (doi:10.1371/journal.pone.0003737)
9. Sukumar M *et al*. 2016 Mitochondrial membrane potential identifies cells with enhanced stemness

for cellular therapy. *Cell Metab.* **23**, 63–76. (doi:10.1016/j.cmet.2015.11.002)

10. Nesin V, Pakhomov AG. 2012 Inhibition of voltage-gated Na+ current by nanosecond pulsed electric field (nsPEF) is not mediated by Na+ influx or Ca2+ signaling. *Bioelectromagnetics* **33**, 443–451. (doi:10.1002/bem.21703)
11. Yamada M *et al*. 2007 Electrical stimulation modulates fate determination of differentiating embryonic stem cells. *Stem Cells* **25**, 562–570. (doi:10.1634/stemcells.2006-0011)
12. Titushkin I, Cho M. 2009 Regulation of cell cytoskeleton and membrane mechanics by electric field: role of linker proteins. *Biophys. J.* **96**, 717–728. (doi:10.1016/j.bpj.2008.09.035)
13. Cheng S-L, Yang JW, Rifas L, Zhang S-F, Avioli LV. 1994 Differentiation of human bone marrow osteogenic stromal cells *in vitro*: induction of the osteoblast phenotype by dexamethasone. *Endocrinology* **134**, 277–286. (doi:10.1210/endo.134.1.8275945)
14. Yamaguchi A, Katagiri T, Ikeda T, Wozney JM, Rosen V, Wang EA, Kahn AJ, Suda T, Yoshiki S. 1991 Recombinant human bone morphogenetic protein-2 stimulates osteoblastic maturation and inhibits myogenic differentiation *in vitro*. *J. Cell Biol.* **113**, 681–687. (doi:10.1083/jcb.113.3.681)
15. Thrivikraman G, Boda SK, Basu B. 2018 Unraveling the mechanistic effects of electric field stimulation towards directing stem cell fate and function: a tissue engineering perspective. *Biomaterials* **150**, 60–86. (doi:10.1016/j.biomaterials.2017.10.003)
16. Xu H, Zhang J, Lei Y, Han Z, Rong D, Yu Q, Zhao M, Tian J. 2016 Low frequency pulsed electromagnetic field promotes C2C12 myoblasts proliferation via activation of MAPK/ERK pathway. *Biochem. Biophys. Res. Commun.* **479**, 97–102. (doi:10.1016/j.bbrc.2016.09.044)
17. Liu M, Lee C, Laron D, Zhang N, Waldorff EI, Ryaby JT, Feeley B, Liu X. 2017 Role of pulsed electromagnetic fields (PEMF) on tenocytes and myoblasts—potential application for treating rotator cuff tears. *J. Orthop. Res.* **35**, 956–964. (doi:10.1002/jor.23278)
18. Nuccitelli R. 1992 Endogenous ionic currents and DC electric fields in multicellular animal tissues. *Bioelectromagnetics* **13**, 147–157. (doi:10.1002/bem.2250130714)
19. Sauer H, Rahimi G, Hescheler J, Wartenberg M. 1999 Effects of electrical fields on cardiomyocyte differentiation of embryonic stem cells. *J. Cell. Biochem.* **75**, 710–723. (doi:10.1002/(SICI)1097-4644(19991215)75:4<710::AID-JCB16>3.0.CO;2-Z)
20. Serena E, Figallo E, Tandon N, Cannizzaro C, Gerecht S, Elvassore N, Vunjak-Novakovic G. 2009 Electrical stimulation of human embryonic stem cells: cardiac differentiation and the generation of reactive oxygen species. *Exp. Cell Res.* **315**, 3611–3619. (doi:10.1016/j.yexcr.2009.08.015)
21. Petrella RA, Mollica PA, Zamponi M, Reid JA, Xiao S, Bruno RD, Sachs PC. 2018 3D bioprinter applied picosecond pulsed electric fields for targeted manipulation of proliferation and lineage specific gene expression in neural stem cells. *J. Neural Eng.* **15**, 056021. (doi:10.1088/1741-2552/aac8ec)
22. Gittens RA, Olivares-Navarrete R, Rettew R, Butera RJ, Alamgir FM, Boyan BD, Schwartz Z. 2013 Electrical polarization of titanium surfaces for the enhancement of osteoblast differentiation. *Bioelectromagnetics* **34**, 599–612. (doi:10.1002/bem.21810)
23. Griffin M, Sebastian A, Colthurst J, Bayat A. 2013 Enhancement of differentiation and mineralisation of osteoblast-like cells by degenerate electrical waveform in an *in vitro* electrical stimulation model compared to capacitive coupling. *PLoS ONE* **8**, e72978. (doi:10.1371/journal.pone.0072978)
24. Zhang J, Li M, Kang E-T, Neoh KG. 2016 Electrical stimulation of adipose-derived mesenchymal stem cells in conductive scaffolds and the roles of voltage-gated ion channels. *Acta Biomater.* **32**, 46–56. (doi:10.1016/j.actbio.2015.12.024)
25. Fujita R, Crist C. 2018 Translational control of the myogenic program in developing, regenerating, and diseased skeletal muscle. *Curr. Top. Dev. Biol.* **126**, 67–98. (doi:10.1016/bs.ctdb.2017.08.004)
26. Gopinath SD, Rando TA. 2008 Stem cell review series: aging of the skeletal muscle stem cell niche. *Aging Cell* **7**, 590–598. (doi:10.1111/j.1474-9726.2008.00399.x)
27. Chopinet L, Rols M-P. 2015 Nanosecond electric pulses: a mini-review of the present state of the art. *Bioelectrochemistry* **103**, 2–6. (doi:10.1016/j.bioelechem.2014.07.008)
28. Zhou P, He F, Han Y, Liu B, Wei S. 2018 Nanosecond pulsed electric field induces calcium mobilization in osteoblasts. *Bioelectrochemistry* **124**, 7–12. (doi:10.1016/j.bioelechem.2018.06.009)
29. Stacey M, Fox P, Buescher S, Kolb J. 2011 Nanosecond pulsed electric field induced cytoskeleton, nuclear membrane and telomere damage adversely impact cell survival. *Bioelectrochemistry* **82**, 131–134. (doi:10.1016/j.bioelechem.2011.06.002)
30. Discher DE, Mooney DJ, Zandstra PW. 2009 Growth factors, matrices, and forces combine and control stem cells. *Science* **324**, 1673–1677. (doi:10.1126/science.1171643)
31. Katsuki S, Moreira K, Dobbs F, Joshi RP, Schoenbach KH. 2002 Bacterial decontamination with nanosecond pulsed electric fields. In *Conf. Proc. of the 25th Int. Power Modulator Symposium, 2002 and 2002 High-Voltage Workshop, June, Hollywood, CA*, pp. 648–651. Piscataway, NJ: IEEE.
32. Chalise PR, Perni S, Shama G, Novac BM, Smith IR, Kong MG. 2006 Lethality mechanisms in *Escherichia coli* induced by intense sub-microsecond electrical pulses. *Appl. Phys. Lett.* **89**, 153902. (doi:10.1063/1.2361271)
33. Nuccitelli R, Pliquett U, Chen X, Ford W, James Swanson R, Beebe SJ, Kolb JF, Schoenbach KH. 2006 Nanosecond pulsed electric fields cause melanomas to self-destruct. *Biochem. Biophys. Res. Commun.* **343**, 351–360. (doi:10.1016/j.bbrc.2006.02.181)
34. Feng J-F, Liu J, Zhang L, Jiang J-Y, Russell M, Lyeth BG, Nolta JA, Zhao M. 2017 Electrical guidance of human stem cells in the rat brain. *Stem Cell Rep.* **9**, 177–189. (doi:10.1016/j.stemcr.2017.05.035)
35. Castle J, Garner AL, Smith R, Davis B, Klopman S, Dinn SR, Torres AS, Neculaes VB. 2018 Hematopoietic stem cell and fibroblast proliferation following platelet electrostimulation. *IEEE Access.* **6**, 56 395–56 401. (doi:10.1109/ACCESS.2018.2872930)
36. Robinson VS, Garner AL, Loveless AM, Neculaes VB. 2017 Calculated plasma membrane voltage induced by applying electric pulses using capacitive coupling. *Biomed. Phys. Eng. Express* **3**, 025016. (doi:10.1088/2057-1976/aa630a)
37. Jiang C, Davalos RV, Bischof JC. 2015 A review of basic to clinical studies of irreversible electroporation therapy. *IEEE Trans. Biomed. Eng.* **62**, 4–20. (doi:10.1109/TBME.2014.2367543)
38. Wu S, Wang Y, Guo J, Chen Q, Zhang J, Fang J. 2014 Nanosecond pulsed electric fields as a novel drug free therapy for breast cancer: an *in vivo* study. *Cancer Lett.* **343**, 268–274. (doi:10.1016/j.canlet.2013.09.032)
39. Garner AL, Caiafa A, Jiang Y, Klopman S, Morton C, Torres AS, Loveless AM, Neculaes VB. 2017 Design, characterization and experimental validation of a compact, flexible pulsed power architecture for *ex vivo* platelet activation. *PLoS ONE* **12**, e0181214. (doi:10.1371/journal.pone.0181214)
40. Yue F, Bi P, Wang C, Li J, Liu X, Kuang S. 2016 Conditional loss of *Pten* in myogenic progenitors leads to postnatal skeletal muscle hypertrophy but age-dependent exhaustion of satellite cells. *Cell Rep.* **17**, 2340–2353. (doi:10.1016/j.celrep.2016.11.002)
41. Kolb JF, Kono S, Schoenbach KH. 2006 Nanosecond pulsed electric field generators for the study of subcellular effects. *Bioelectromagnetics* **27**, 172–187. (doi:10.1002/bem.20185)
42. Frey W, White JA, Price RO, Blackmore PF, Joshi RP, Nuccitelli R, Beebe SJ, Schoenbach KH, Kolb JF. 2006 Plasma membrane voltage changes during nanosecond pulsed electric field exposure. *Biophys. J.* **90**, 3608–3615. (doi:10.1529/biophysj.105.072777)
43. Vadlamani A, Detwiler DA, Dhanabal A, Garner AL. 2018 Synergistic bacterial inactivation by combining antibiotics with nanosecond electric pulses. *Appl. Microbiol. Biotechnol.* **102**, 7589–7596. (doi:10.1007/s00253-018-9215-y)